

# Biologically-Based Modeling Of Anthrax Infection: Modulation Of Macrophage MAPK Signaling Pathway By Lethal Toxin

Peter J. Robinson<sup>1\*</sup>, Emily J. Fleming<sup>1</sup>, C. Eric Hack<sup>1</sup>, Daniel J. Schneider<sup>2</sup>, Jeffery M. Gearhart<sup>1</sup>

<sup>1</sup> Air Force Research Laboratory, AFRL, Wright-Patterson AFB, OH USA .

<sup>2</sup> Air Force Institute of Technology, AFIT, Wright-Patterson AFB, OH USA .

Current address: US Air Force School of Aerospace Medicine, USAFSAM, Brooks City-Base, TX USA.

\* Corresponding Author: Tel: 937-904-9502 | Fax: 937-255-1474 | Email: peter.robinson@wpafb.af.mil

**Suggested citation:** Robinson, P; Fleming, E; Hack, C; Schneider, D; Gearhart, J (2010) "Biologically-Based Modeling Of Anthrax Infection: Modulation Of Macrophage MAPK Signaling Pathway By Lethal Toxin", JMedCBR 8, 4 September 2010, [http://www.jmedcbr.org/issue\\_0801/PJRobinson/PJRobinson\\_09\\_10.html](http://www.jmedcbr.org/issue_0801/PJRobinson/PJRobinson_09_10.html).

## ABSTRACT

To a large extent, *Bacillus anthracis*, etiologic agent of anthrax, owes its virulence to the production of the multicomponent anthrax toxin that mediates the toxigenic stage of infection. One toxin component, lethal factor (LF), cleaves most isoforms of mitogen-activated protein kinase (MAPK)-kinases (MAPKKs) close to their N-terminus. This interferes with a major signaling pathway linking the activation of membrane receptors, such as toll-like receptors, to the transcription of several genes, including those encoding pro-inflammatory cytokines, as well as the p38 MAPK dependent expression of pro-survival genes. LF gains access to the host cell cytosol after it is secreted by newly germinated spores (vegetative bacteria, early infection) or after it is endocytosed from the systemic circulation during toxemia (later, systemic infection). In either case, translocation of LF from the endosome to the cytosol is mediated by pores formed by another secreted toxin component, protective antigen (PA). We have developed an initial model for the interaction of LF with host macrophages. We translate existing parameterized models of the MAPK pathway from Systems Biology Markup Language (SBML) into Berkeley Madonna™, a format suitable for integrated physiologically-based modeling of both anthrax proliferation and host system response. MAPKK cleavage by LF leads to a decline (to zero) in the signaling output that has a characteristic half-time that can be correlated with the net potency of the toxin, as exemplified by reductions in macrophage viability *in vitro* in a number of studies. A kinetic model that simulates the accumulation of LF in the macrophage cytosol over time, in combination with a proliferation model that simulates LF dosimetry, and a description of the cellular response to signal reduction (alterations in gene expression leading to changes in cytokine production, apoptosis etc.), provides a model

framework that predicts the time-course of the physiological effects of anthrax lethal toxin in biologically varied individuals.

## INTRODUCTION

Inhalation anthrax is an often fatal disease of bioterrorism significance in which macrophages play key roles in the disease process. Initially, alveolar macrophages engulf *Bacillus anthracis* spores, which germinate into vegetative, toxin producing bacteria as they are transported to the regional lymph nodes; these bacteria are released into circulation by apoptotic macrophages that fail to elicit a pro-inflammatory response at this early stage of infection [Ross, 1957; Guidi-Rontani *et al.*, 1999; Pellizzari *et al.*, 1999]. Exponential growth of vegetative *B. anthracis* in the blood stream leads to systemic anthrax during which toxins accumulate to high levels, culminating in sudden shock caused by tumor necrosis factor (TNF)- $\alpha$  and interleukin (IL)-1 secreted, in part, by necrotic macrophages [Gutting *et al.*, 2005; Dixon *et al.*, 1999]. Macrophages may not be the only phagocytic cells important in the early stage of inhalation anthrax, however. Lung dendritic cells may also play a role in transporting *B. anthracis* spores to the thoracic lymph nodes [Cleret *et al.*, 2007], during which process they are also susceptible to toxin impairment [Agrawal *et al.*, 2003].

Among the key virulence factors of *B. anthracis* is production of the binary toxins, lethal toxin (LT) and edema toxin (ET). Each toxin is composed of an enzyme, lethal factor (LF) in the case of LT and edema factor (EF) in the case of ET, and a pore-forming protein, protective antigen (PA). PA heptamerizes with other PA molecules at host cell membrane receptors and translocates EF and/or LF into the host cell's cytosol where they exert their toxic effects [Bradley *et al.*, 2001]. EF is an adenylate cyclase that increases cyclic adenosine monophosphate (AMP) levels, resulting in tissue edema [Leppla, 1982] whereas LF is a metalloprotease that cleaves most isoforms of mitogen-activated protein kinase (MAPK)-kinases (MAPKKs) close to their N-terminus [Duesbery *et al.*, 1998; Vitale *et al.*, 1998]. There are a number of MAPK signaling pathways that are important components of an effective innate immune response to infection, and MAPKKs are important intermediates in linking macrophage activation at membrane receptors to these MAPK pathways. In an LF concentration-dependent fashion, MAPKK cleavage by LF in activated macrophages leads to apoptosis by inhibiting the p38 MAPK signaling pathway [Park *et al.*, 2002] and impaired pro-inflammatory response, due to inhibition of genes encoding them (reviewed in [Ono and Han, 2000]). Thus the apoptotic death of macrophages and the absence of a pro-inflammatory response contribute to the impaired immune response to early *B. anthracis* infection and the subsequent progression to bacteremia and fatal toxemia that rapidly ensue after vegetative *B. anthracis* are released into circulation.

The current paper is part of a larger program to develop a suite of mechanism-based quantitative models that describe anthrax infection, from spore deposition in the lung to the final stages of bacteremia [Robinson *et al.*, 2009]. The purpose of such a multi-level model is to be able to predict the response of the host organism (including humans) to specific anthrax exposure conditions. Each individual module in the larger model will be separately developed and validated as far as possible in the light of appropriate *in vitro* and *in vivo* data. As part of this program we are developing spore deposition models for a number of animal species, including rabbits and humans [Hack *et al.*, 2009]. We are also developing models that quantitate the response of the host

immune system and predict the time-course for circulating levels of PA and LF [Fleming *et al.*, 2009], as well as *B. anthracis* themselves. The current paper describes a key part of this overall process in that it focuses on the initial interaction of the macrophage with the deposited spore in the lung and the subsequent subversion of macrophage internal signaling machinery for the macrophage's own purposes.

## MODEL FOR THE DISRUPTION OF THE MAPK SIGNALING PATHWAY

A simple model of the toxigenic phase of anthrax was developed. The diagram of the macrophage and its interaction with *B. anthracis* and LT in figure 1 is presented to demonstrate this model (figure 1). Figure 1 also shows how the macrophage compartment is linked to other anthrax sub-models being developed in our laboratory [Hack *et al.*, 2009 and Fleming *et al.*, 2009].

In the present paper, we focus our modeling effort on the interaction of LF in the cytosol with the MAPK signaling pathway. Figure 2 illustrates the MAPK signaling cascade adapted to the present context of interaction with *B. anthracis*. The MAPK pathway itself is based on the Kholodenko model [Kholodenko, 2000]. This is one of the simplest representations of the MAPK cascade in the literature. Rates for the numbered reactions in figure 2 are given in the model code in the Appendix as J1 through J10, where MAPKK and MAPKK-kinase (MAPKKK) are rewritten as MKK and MKKK, etc. Schneider [Schneider, 2008] has examined a number of alternative parameterized and validated MAPK models in this context [Huang and Ferrell, 1996; Levchenko *et al.*, 2000] and has concluded that they behave similarly (see Conclusions below). We translate the existing fully parameterized model of the MAPK pathway of Kholodenko from Systems Biology Markup Language (SBML) (available at [www.ebi.ac.uk/biomodels](http://www.ebi.ac.uk/biomodels)) into Berkeley Madonna™, a format suitable for integrated physiologically-based modeling of both anthrax proliferation and host system response. We then add specific interactions of this pathway with *B. anthracis* as outlined below in figure 2.

In the cellular response to pathogens, the interaction of *B. anthracis* with receptors on the macrophage outer membrane activates the MAPK cascade, providing the “input” stimulus to the signaling pathway. We assume that this manifests itself as an increase in the maximal rate  $V1$  for the phosphorylation of MAPKKK (figure 2). This input stimulus to the system is carried through the signaling cascade, resulting in an enhanced output in the form of increased MAPK-PP (double phosphorylated MAPKK) levels that reflect the stimulus. The increased MAPK-PP levels in turn regulate the expression of various genes involved in the innate immune response such as the production and release of pro-inflammatory cytokines (figure 3).

In the presence of LT, MAPKK, MAPKK-P (phosphorylated MAPKK) and MAPKK-PP are cleaved by cytosolic LF. This cleavage disrupts the Extracellular Signal-Regulated Kinase (ERK) and p38 signaling pathways, subsequently inhibiting the production of pro-inflammatory cytokines TNF- $\alpha$ , IL-1, and IL-6 [Erwin *et al.*, 2001] whose gene expression were initially induced in the activated macrophage. In addition, MAPKK cleavage leads to macrophage apoptosis, which is normally suppressed in the activated macrophage [Bardwell *et al.*, 2004]. Finally, it appears that due to the MAPK pathway's involvement in processes critical for cell maintenance and survival, these processes may also be disrupted (presumably as the LF decreases the signaling output

to levels below the original “maintenance baseline” before exposure to anthrax), resulting in macrophage necrosis. Combining apoptosis and necrosis (despite their different infection time-scales), we thus make the general assumption in fitting our model to cell viability data that the output signal can be compared directly with macrophage cell viability (figure 3). This assumption is supported by experimental studies in which mechanisms and timelines of cell death are dependent upon macrophage sensitivity to LF and cytosolic LF concentration (reviewed in [Moayeri *et al.*, 2009]).

We assume further that the total mass of MAPK is conserved, or at least maintained by a basal synthesis rate. Cleavage by LF leads to decreases in total MAPKs, which ultimately cannot be sufficiently replenished by synthesis. We initially assume first-order removal of MAPKK, MAPKK-P and MAPKK-PP with rate constants  $KX$ ,  $KXP$  and  $KXPP$  ( $s^{-1}$ ), respectively, so that the rate equations (see appendix) for MAPKK, MAPKK-P and MAPKK-PP become:

$$\begin{aligned} \text{MKK}' &= -J3 + J6 - JX \\ \text{MKK\_P}' &= +J3 - J4 + J5 - J6 - JXP \\ \text{MKK\_PP}' &= +J4 - J5 - JXPP \end{aligned} \quad \text{Equation set (1)}$$

where

$$\begin{aligned} J3 &= k3 * \text{MKKK\_P} * \text{MKK} / (\text{KK3} + \text{MKK}) \\ J4 &= k4 * \text{MKKK\_P} * \text{MKK\_P} / (\text{KK4} + \text{MKK\_P}) \\ J5 &= V5 * \text{MKK\_PP} / (\text{KK5} + \text{MKK\_PP}) \\ J6 &= V6 * \text{MKK\_P} / (\text{KK6} + \text{MKK\_P}) \\ JX &= KX * \text{MKK} \\ JXP &= KXP * \text{MKK\_P} \\ JXPP &= KXPP * \text{MKK\_PP} \end{aligned} \quad \text{Equation set (2)}$$

are reaction rates (units of nM/s), and concentrations, MKK, MKK\_P and MKK\_PP, are in nM.

## RESULTS

In our simulations, when there are no *B. anthracis* or toxins present (basal state, no stimulation), for the parameter set given in Kholodenko [Kholodenko, 2000] (see appendix), MAPK levels remain high (at around 300 nM), while the output for the MAPK-PP levels quickly falls to zero. However, when the same pathway is subjected to stimulation, due, for example, to the presence of anthrax spores, a characteristic oscillatory output in MAPK-PP is obtained, as described in Kholodenko [Kholodenko, 2000]. This oscillatory output is a direct result of the feedback inhibition loop in the Kholodenko model, and is not a feature of all MAPK models, such as those of Huang and Ferrell [Huang and Ferrell, 1996]. In addition, such oscillatory responses are characteristic of simulations of single macrophages, and will be “averaged out” when populations of unsynchronized cells are considered.

External stimulation is represented in this model by the value of  $V1$ , the maximum activation (phosphorylation) rate of MAPKKK (see appendix). If, for example,  $V1$  is increased 20-fold, from its basal rate of 0.125 nM/s to 2.5 nM/s, the output signal oscillates between about 40 and 300 nM of MAPK-PP. Based on the assessment of

Kholodenko [Kholodenko, 2000], such an increase in  $V1$  is assumed in our model to be typical of the upregulation of the MAPK response in the macrophage due to the presence of a bacterial trigger. At this point we do not consider any graduated “dose-response” of the host immune cell to stimuli of varying magnitude.

Addition of LF produced by *B. anthracis*, which cleaves the MAPKK beyond the ability of the host to replenish it, leads to the decline of this oscillatory output, eventually to zero (see figure 4). This decline occurs with the characteristic half-time being determined by the magnitude of the first order rate constants  $KX$ ,  $KXP$ , and  $KXPP$  for MAPKK, MAPKK-P, and MAPKK-PP cleavages, respectively (figure 2). We assume, for simplicity that  $KX$ ,  $KXP$  and  $KXPP$  are equal in magnitude, as it appears that cytotoxic activity does not appear to be related to the phosphorylation state of the MAPKK [Schneider, 2008].

Since the signaling output is assumed to be correlated with the viability of the macrophages (see Methods), we can fit  $KX$  to the cell viability data. Gutting *et al.* [Gutting *et al.*, 2005] cultured murine macrophage cell-lines, IC-21 (LT-resistant), RAW264.7 (LT-sensitive) and J774A.1 (LT-sensitive), in media alone or with *B. anthracis* V1B strain. Macrophage viability was measured by trypan blue exclusion at various times after *B. anthracis* exposure. Figure 4 shows the experimental data (solid circles) and the simulated MAPK-PP signals (oscillating lines) for LT-sensitive macrophages, RAW264.7 and J774A.1. Note that we have time-shifted the cell viability data by five hours, to take into account the time-lag between the introduction of *B. anthracis* and the production of LF toxin. The dotted curves represent model-predicted mean MAPK-PP concentrations, averaged over the oscillations. We assume that cell viability is 100% (horizontal dotted line) before *B. anthracis* is introduced, and this corresponds to a mean concentration of 190 nM MAPK-PP in our model. This estimate takes into account the fact that the cell spends slightly more time at the upper part of the oscillation than the lower part.

If we assume that non-linearities in the system are accounted for by the MAPK cascade, and assume that cell response (viability) is linearly related to MAPK-PP levels, reasonable fits to each set of cell viability data can be obtained with values of  $KX$  ( $=KXP = KXPP$ ) =  $2.9 \times 10^{-4} \text{ s}^{-1}$  and  $1.2 \times 10^{-4} \text{ s}^{-1}$ , respectively for RAW264.7 and J774A.1 macrophages. These fits are accomplished by eye, fitting the average output values (dotted line) to the cell viability data points in figure 4(a) and (b), respectively. Note that this fitted value is the only adjustable parameter in the model.

A similar analysis can be performed for macrophages exposed directly to purified LF and PA. Pellizzari *et al.* exposed RAW264.7 macrophages to 200 ng/mL each of LF and PA and assessed viability using an MTT assay [Pellizzari *et al.*, 1999]. Muehlbauer *et al.* estimated cell viability data for various macrophage cell types using the MTT assay after cells were exposed to 500 ng/mL PA and 250 ng/mL LF [Muehlbauer *et al.*, 2007]. Approximate fitted  $KX$  values for Kholodenko’s MAPK model [Kholodenko, 2000], modified to include cleavage of MAPKK by anthrax LF, are given in table 1 for both these sets of experimental results. Figure 5 shows the modified Kholodenko model fitted to the data of Pellizzari *et al.* Second-order rate constants ( $K2X_{eff}$ ) are also given in table 1 and discussed in greater detail in the Discussion and Conclusions section.

## DISCUSSION AND CONCLUSIONS

The present model describes some aspects of the interaction between *B. anthracis* and the macrophages of the host system. It provides an initial description of the effect of the release of anthrax toxins, specifically LT, on a particular biochemical pathway in the macrophage – the MAPK signaling pathway. As such, it provides a framework for understanding the impact of anthrax on the host system and how the host system's defense mechanisms are co-opted for the benefit of the invading organism. The model of necessity makes a number of simplifying assumptions about a very complex process. The choice of assumptions for any model is always somewhat arbitrary, and, in many cases, may need to be modified as the model is tested in the real world. We believe, however, that the present model is a reasonable first approximation in such an iterative model-building process. It appears to be successful as a proof of the concept that such a complex biological interaction can be modeled down to the molecular level, and the results compare quantitatively with gross observations, such as cell viability and death.

We have focused the present paper on the modulating effect of LF, rather than EF, on the signaling machinery of the host cell. EF acts as a calcium anion and calmodulin dependent adenylate cyclase that greatly increases the level of cyclic AMP in the cell. This increase in cyclic AMP upsets water homeostasis, throws the intracellular signaling pathways off balance, and impairs macrophage function, allowing the bacteria to further evade the immune system. It is envisaged that in our final composite model, the effects of EF will also be taken into account. In the meantime, the adverse effects of *B. anthracis* on macrophage viability are entirely attributed to LF.

The effects of LF on macrophage viability are themselves far from simple. As noted in the introduction, MAPKK cleavage disrupts the ERK and p38 signaling pathways inducing apoptosis. In addition, due to the MAPK pathway's involvement in processes critical for cell maintenance and survival, these processes may also eventually be disrupted resulting in macrophage necrosis. In our model, despite their likely different time-scales, we have combined the effects of apoptosis and necrosis by our estimate of a single rate constant  $KX$  for macrophage viability from *in vitro* data. While this is clearly an over-simplification, we believe it provides an initial interpretation of the data in terms of a single parameter that captures the essence of the macrophage's response to LF.

The present model makes use of a specific, and rather simple, model for the MAPK pathway itself [Kholodenko, 2000]. Other MAPK models are available, and the question naturally arises: do they make a difference as far as the simulated biological response goes? This question has been explored in detail by Schneider [Schneider, 2008], who modified three published MAPK models to reflect this signal inhibition and to estimate a first-order reaction rate by fitting the models to the data of Gutting *et al.* [Gutting *et al.*, 2005]. Table 2 shows a comparison of first-order rate constants  $KX$ ,  $KXP$  and  $KXPP$  (assumed equal to each other: see Results above) for the interaction of *B. anthracis* with RAW264.7 and J774A.1 macrophages, each fitted to the data of Gutting *et al.* [Gutting *et al.*, 2005], for four different MAPK models. These models are the “ultrasensitivity” model of Huang and Ferrell [Huang and Ferrell, 1996], the “negative feedback” models of Kholodenko [Kholodenko, 2000] (with two values for the strength of the negative feedback loop,  $n = 1$  and  $2$  in table 2), and the “scaffold protein” model of

Levchenko *et al.* [Levchenko *et al.*, 2000]. Details of these models are beyond the scope of the present short paper (see [Schneider, 2008] for details); however, it should be noted that the estimated rate constants show a reasonably consistent performance by the models in estimating values for the LF-MAPKK reaction rate parameter for each macrophage type. Additionally, the ratio of rate constants for the two macrophage lines is approximately the same, around 2.3 to 2.4.

Thus, despite different underlying parameters and values, the models displayed consistent behavior, due to the highly conserved signal pathway structure, and provide approximately equal rate constants and measures of the relative sensitivity between cell lines. These results demonstrate model robustness and an ability to guide experimental design toward quantifying the LF reaction rate and estimating the sensitivity of human alveolar macrophages. This in turn is an essential step in extrapolating such models to estimate the likely human response to anthrax exposure.

Up to this point, the degree of interaction between *B. anthracis* and the macrophage has been described in terms of a first-order rate constant  $KX$ . In reality, this parameter is not fixed, but depends on the LF concentration in the macrophage cytosol,  $[LF]_c$  in figure 1. It can better be described as a product of a "true" second order rate constant,  $K2X$ , multiplied by  $[LF]_c$ , which typically increases with time (and in the Gutting experiments is probably zero for the first five hours or so).

In some *in vitro* experiments in which PA is in excess, we may assume that  $[LF]_c$  is to some extent reflected by  $[LF]$ , the LF concentration in the surrounding medium. In such cases, an "effective" second-order rate constant  $K2X_{eff}$  can be calculated by dividing the fitted  $KX$  value by  $[LF]$ . Such calculated values for  $K2X_{eff}$  are given in table 1 for the data of Pelizzari *et al.* and Muehlbauer *et al.* and take into account, albeit crudely, the different LF concentrations in the medium. Values of  $K2X_{eff}$  thereby provide a better indication of the sensitivity or susceptibility of the particular macrophage type to LF than do values for  $KX$ . As the model is further refined to specifically take into account the accumulation of LF in the cytosol, more accurate second-order rate constants (and relative susceptibilities) can be calculated.

Using our model,  $[LF]_c$  is due to the translocation of LF by PA pores in the endosomal membrane of the host cell. LF and PA arrive in the endosome by one of two routes (see figure 1 above). Firstly, LF and PA are secreted by viable bacteria that have germinated from endocytosed spores as described above. Secondly, LF and PA may be endocytosed directly from the extracellular fluid as part of a receptor-bound complex. For macrophages in the initial stages of an infection, and before circulating concentrations of exotoxins have had time to accumulate, the first process (secretion of toxins by endocytosed bacteria) is by far the most important. However, for other tissues of the body, and at later times for macrophages as well, the second process (direct endocytosis of toxins) is likely to dominate, and likely forms a major pathway for peripheral cell death and tissue damage, ultimately leading to the demise of the host, in some cases. Both these processes will come into play when we extend the present model to link it with a model we are currently developing for *B. anthracis* deposition and proliferation via  $[LF]_c$ .

Differences in sensitivity of macrophages to anthrax LT, depending upon their genetic background, have been demonstrated by Muehlbauer *et al.* [Muehlbauer *et al.*, 2007]. Bone marrow derived macrophages (BMM) from DBA/2, AKR and C57BL/6

mice and human monocyte-derived macrophages, previously described as LT resistant, were efficiently killed following LT treatment slowly by apoptosis. BMMs derived from BALB/c and C3H/HeJ mice, described as LT-sensitive, were in contrast killed rapidly by necrosis. Further, LT-sensitive murine macrophage cell lines exposed to sublytic concentrations of LT die by apoptosis rather than the necrosis induced by saturating LT exposure concentrations [Park *et al.*, 2002]. These differences can be quantified in terms of the present model via the characteristic rate constant  $KX$  (table 1).

The present model can be extended to higher levels of model organization. For example, we may model germinated spores in macrophages as sources of LF, and model the multiplication of vegetative bacteria within macrophages. It has been shown, for example, that spore germination may take place within minutes of endocytosis [Guidi-Rotani *et al.*, 1999]. Similarly, the bactericidal activity of alveolar macrophages against *B. anthracis* spores [Ribot *et al.*, 2006] can be modeled. To complete the description, we will link the current toxigenic LF-MAPK model to the spore lung deposition model also being developed in our laboratory. The latter model includes deposition of anthrax spores in the respiratory tract, phagocytosis by alveolar macrophages and transport of macrophages to the lymph nodes (see figure 1). We need to compare and combine the transport and proliferation of the key components of this system to give a quantitative framework for disease progression: where do macrophages go in the body, how long does it take to get there compared with the proliferation of anthrax bacteria within them, and at which point are the macrophages killed by the release of toxins within and exposure to toxins without? Such a comprehensive model can be used in risk assessment and in the design and assessment of existing and new therapies. Thus, when combined with the proliferation model that simulates LF dosimetry, and with a description of the biological effect of signal reduction in terms of the cellular response (alterations in gene expression leading to changes in cytokine production, apoptosis etc.), we will have a model framework that begins to predict the time-course of the biological effects of anthrax exposure in biologically varied individuals. In addition, model predictions can be compared with observations, allowing the model to be validated and, if necessary, modified.

FIGURES

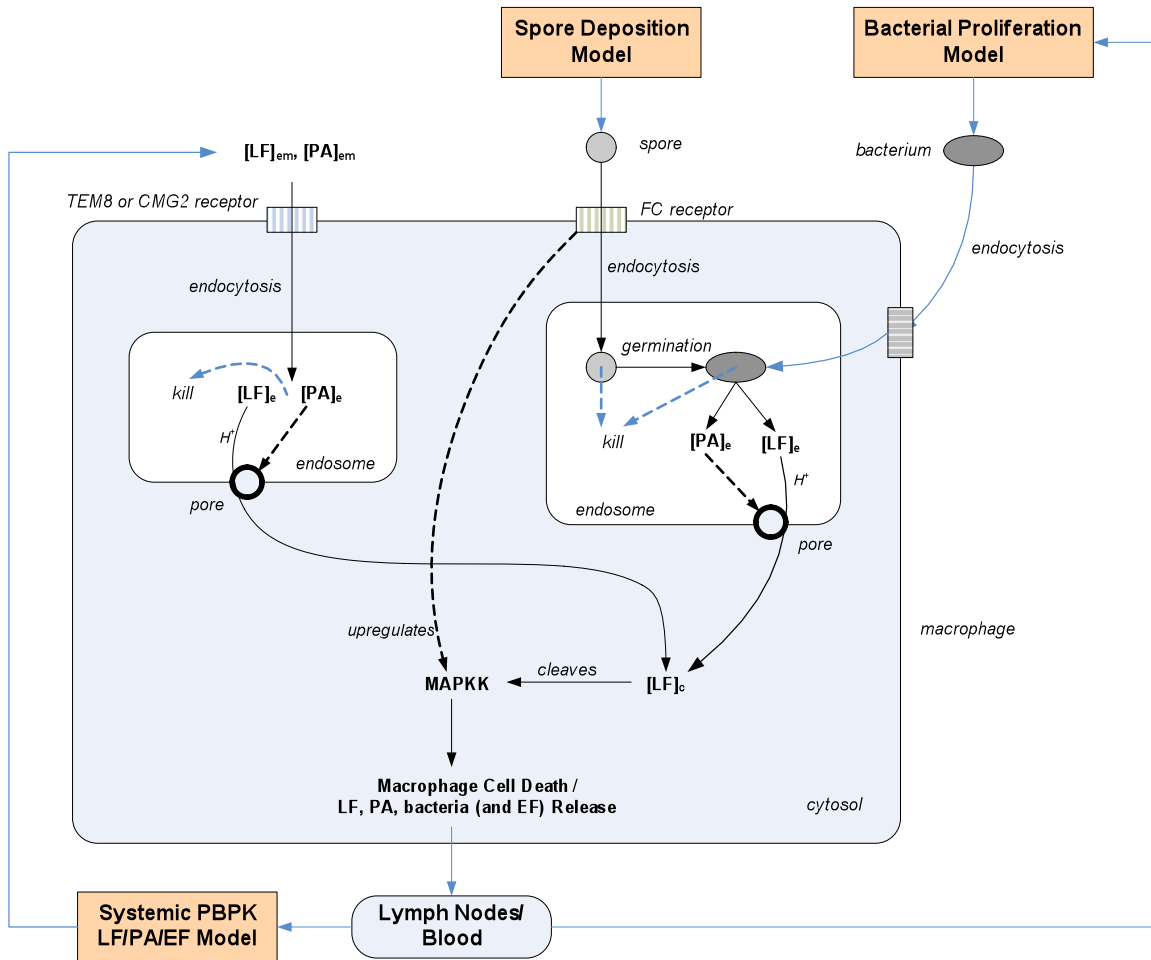
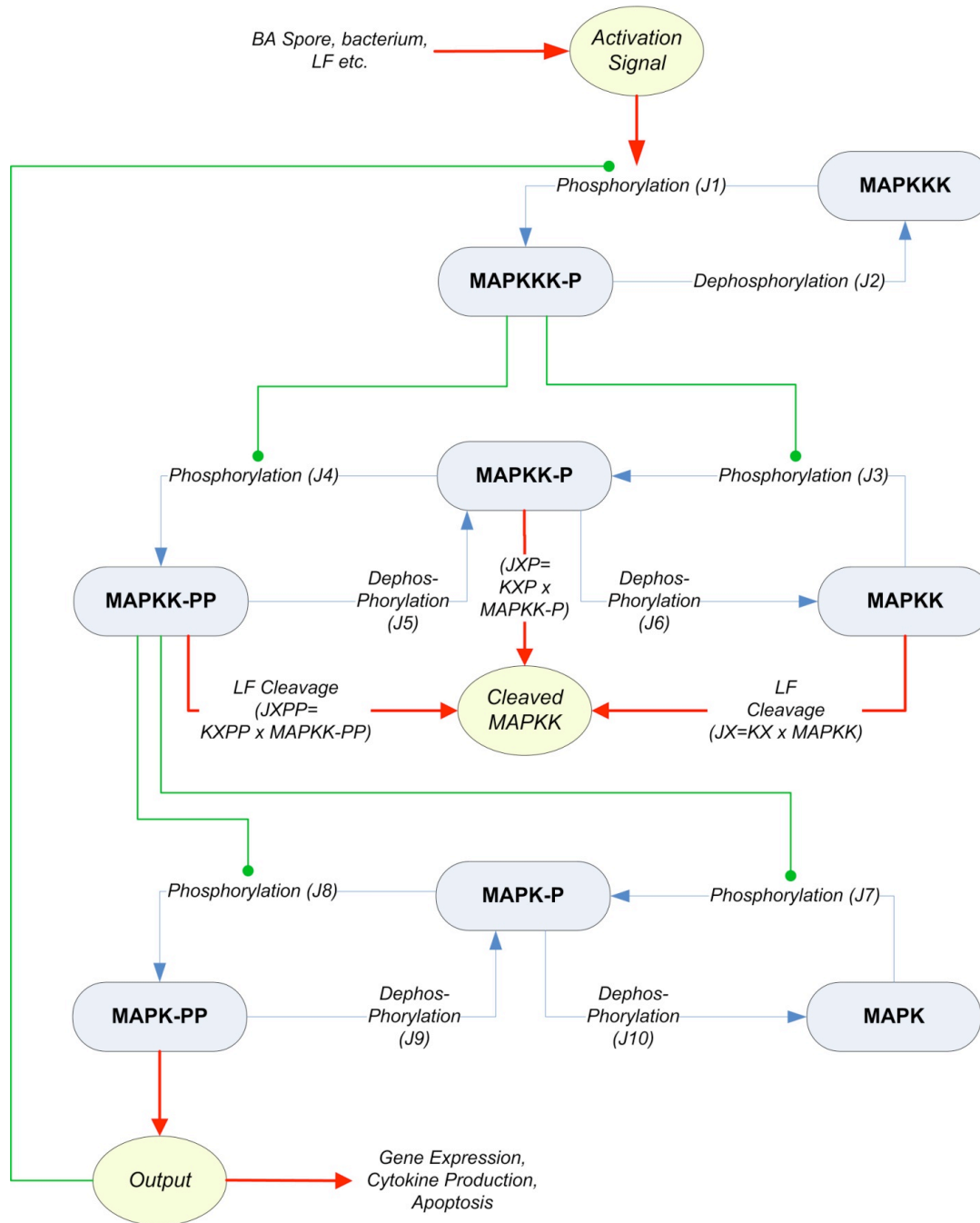
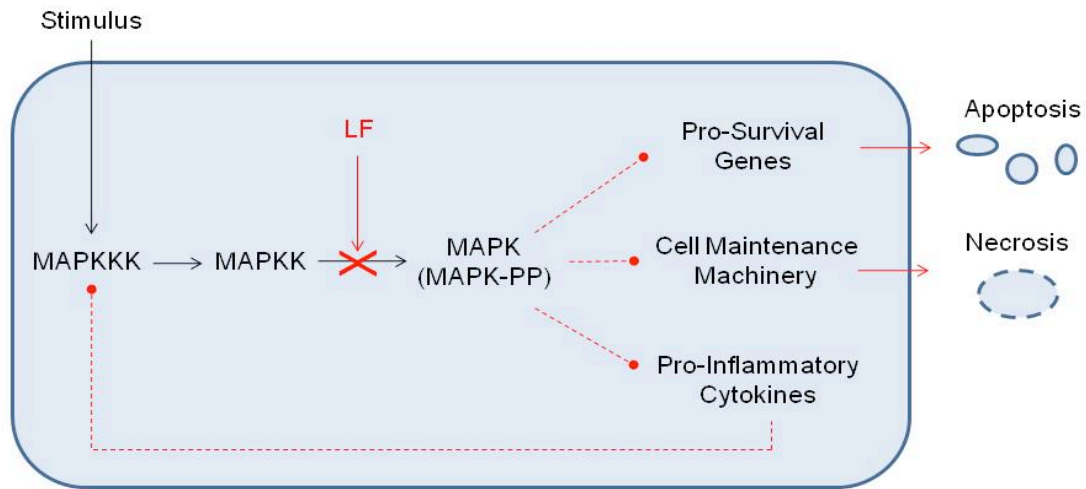


Figure 1. Simplified schematic of the interaction of *B. anthracis* with macrophages, culminating in the disruption of the MAPK signaling pathway by LF in the cytosol, cell death, and bacteria/toxin release.



**Figure 2: Model graph, from Kholodenko (2000), adapted from BioModels repository, European Bioinformatics Institute (EMBL-EBI). This graphic illustrates the MAPK signaling cascade model as applied to the interaction with *B. anthracis*. Equations for the phosphorylation/dephosphorylation rates J1 through J10 are given in the Appendix. The cleavage rates JX, JXP and JXPP by anthrax LF are given respectively by the products of first-order rate constants KX, KXP and KXPP and the concentrations of MAPKK, MAPKK-P and MAPKK-PP (red arrows).**



**Figure 3. Disruption of the MAPK signaling cascade by LF leads to diminishing, and eventual absence, of the output signal, which corresponds with cell death.**

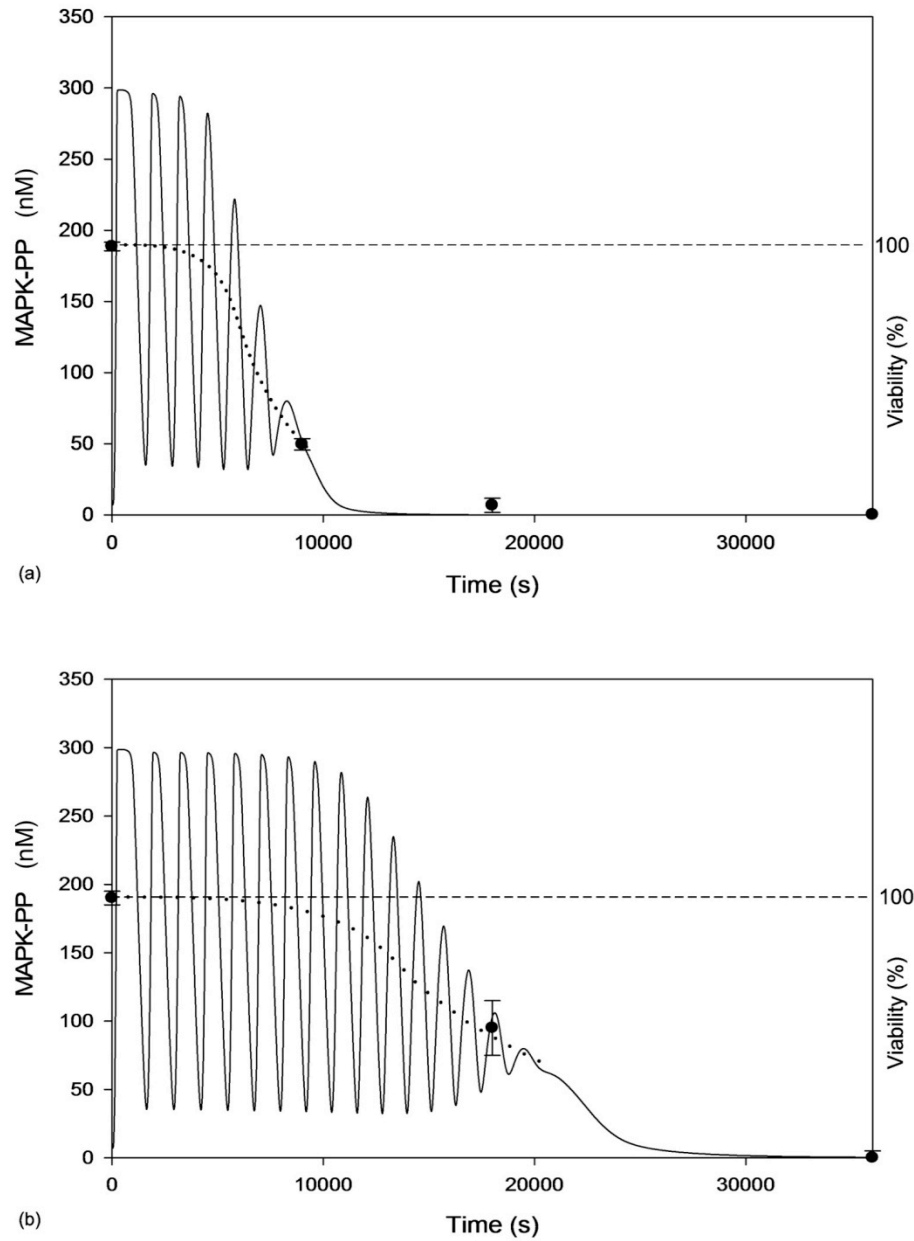


**Figure 4. Experimental data (solid circles) and the simulated MAPK-PP signals (oscillating lines) for LT-sensitive macrophages, RAW264.7 (a) and J774A.1 (b). The cell viability data are from Gutting *et al.* [Gutting *et al.*, 2005] (mean +/- standard error, n=8). The predicted output is from the MAPK model of Kholodenko [Kholodenko, 2000], modified to include cleavage of MAPKK by anthrax LF via a first-order rate constant,  $KX$ . Fitted to  $KX$  values are  $2.9 \times 10^{-4} \text{ s}^{-1}$  (a) and  $1.2 \times 10^{-4} \text{ s}^{-1}$  (b)**

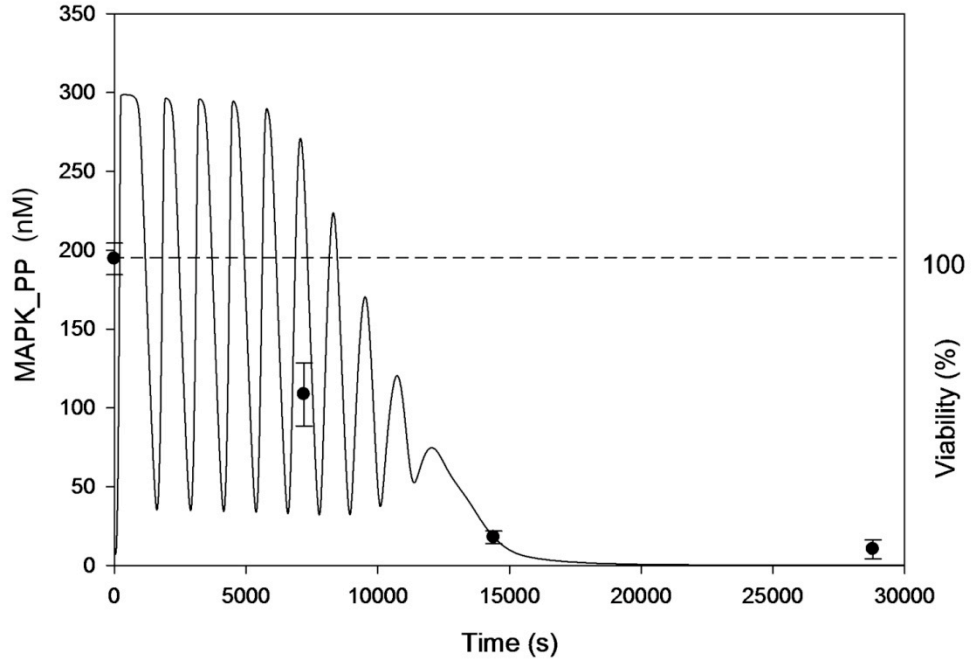


**Figure 5.** Predicted output from the MAPK model of Kholodenko [Kholodenko, 2000], modified to include cleavage of MAPKK by anthrax LF via a first-order rate constant  $KX$  (set here to  $2.0 \times 10^{-4} \text{ s}^{-1}$ ), and compared with RAW264.7 cell viability data from Pellizzari *et al.*, 1999.

**TABLES**

**Table 1. Rate constants  $KX$  and  $K2X_{eff}$  for the interaction of specific combinations of LF and PA with various macrophage cell types *in vitro***

| <b>Macrophage Type/Source</b> | <b>LF Conc. (ng/mL)</b> | <b>PA Conc. (ng/mL)</b> | <b><math>KX</math> (<math>s^{-1}</math>) (fitted)</b> | <b><math>K2X_{eff}</math> (ng/ml/s) §</b> | <b>Data Reference</b>           |
|-------------------------------|-------------------------|-------------------------|---|---|---------------------------------|
| RAW264.7                      | unk.                    | unk.                    | $2.9 \times 10^{-4}$                                  | -   | Gutting <i>et al.</i> , 2005    |
| J774A.1                       | unk.                    | unk.                    | $1.2 \times 10^{-4}$                                  | -   | Gutting <i>et al.</i> , 2005    |
| RAW264.7                      | 200                     | 200                     | $2.0 \times 10^{-4}$                                  | $1.0 \times 10^{-6}$                      | Pellizzari <i>et al.</i> , 1999 |
| BALB/C                        | 250                     | 500                     | $4.5 \times 10^{-4}$                                  | $1.8 \times 10^{-6}$                      | Muehlbauer <i>et al.</i> , 2007 |
| C3H                           | 250                     | 500                     | $4.5 \times 10^{-4}$                                  | $1.8 \times 10^{-6}$                      | Muehlbauer <i>et al.</i> , 2007 |
| AKR                           | 250                     | 500                     | $1.0 \times 10^{-5}$                                  | $4.0 \times 10^{-8}$                      | Muehlbauer <i>et al.</i> , 2007 |
| BL/6*                         | 250                     | 500                     | $1.2 \times 10^{-5}$                                  | $4.8 \times 10^{-8}$                      | Muehlbauer <i>et al.</i> , 2007 |
| DBA                           | 250                     | 500                     | $1.4 \times 10^{-5}$                                  | $5.6 \times 10^{-8}$                      | Muehlbauer <i>et al.</i> , 2007 |
| Human                         | 250                     | 500                     | $1.1 \times 10^{-5}$                                  | $4.4 \times 10^{-8}$                      | Muehlbauer <i>et al.</i> , 2007 |

\*Two separate experiments with BL/6 derived macrophages were reported.

unk = unknown

§An effective second order rate constant (calculated as  $KX/[LF]$ , see Discussion and Conclusions)

**Table 2. Comparison of first-order rate constants  $KX$ ,  $KXP$  and  $KXPP$  (assumed equal to each other) for the interaction of *B. anthracis* with RAW264.7 and J774A.1 macrophages, each fitted to the data of Gutting *et al.* [Gutting *et al.*, 2005], for four different MAPK models\***

| <b>Macrophage Cell Line</b> | <b>Ultrasensitivity [Huang, 1996]</b> | <b>Negative Feedback [Kholodenko, 2000]</b> |                             | <b>Scaffold [Levchenko, 2000]</b> |
|-----------------------------|---------------------------------------|---|-----------------------------|-----------------------------------|
|                             |                                       | <b>n = 1</b>                                | <b>n = 2</b>                |                                   |
| RAW264.7                    | $2.95 \times 10^{-4} s^{-1}$          | $2.9 \times 10^{-4} s^{-1}$                 | $2.3 \times 10^{-4} s^{-1}$ | $5.9 \times 10^{-4} s^{-1}$       |
| J774A.1                     | $1.3 \times 10^{-4} s^{-1}$           | $1.2 \times 10^{-4} s^{-1}$                 | $9.5 \times 10^{-5} s^{-1}$ | no fit                            |
| Ratio                       | 2.3                                   | 2.4   | 2.4                         | n/a                               |

\*These models are the “ultrasensitivity” model of Huang and Ferrell [Huang and Ferrell 1996], the “negative feedback” models of Kholodenko [Kholodenko, 2000] and the “scaffold protein” model of Levchenko *et al.* [Levchenko *et al.*, 2000]

## REFERENCES

- Agrawal, 2003. Agrawal, A., Lingappa, J., Leppla, S.H., Agrawal, S., Jabbar, A., Quinn, C. and Pulendran, B. (2003) Impairment of dendritic cells and adaptive immunity by anthrax lethal toxin. *Nature* 424, 329-334.
- Bardwell, 2004. Bardwell, A.J., Abdollahi, M., and Bardwell, L. (2004) Anthrax lethal factor-cleavage products of MAPK (mitogen-activated protein kinase) kinases exhibit reduced binding to their cognate MAPKs. *Biochem J.* 378, 569-577.
- Bradley, 2001. Bradley, K.A., Mogridge, J., Mourez, M., Collier, R.J., and Young, J.A.T. (2001) Identification of the cellular receptor for anthrax toxin. *Nature.* 414, 225-229.
- Cleret, 2007. Cleret, A., Quesnel-Hellmann, A., Vallon-Eberhard, A., Verrier, B., Jung, S., Vidal, D., Mathieu, J., and Tournier, J.N. (2007) Lung dendritic cells rapidly mediate anthrax spore entry through the pulmonary route. *J Immunol.* 178, 7994–8001.
- Dixon, 1999. Dixon, T.C., Meselson, M., Guillemin, J., Hanna, P.C. (1999) Anthrax. *N Engl J Med.* 341, 815-826.
- Duesbery, 1998. Duesbery, N.S., Webb, C.P., Leppla, S.H., Gordon, V.M., Klimpel, K.R., Copeland, T.D., Ahn, N.G., Oskarsson, M.K., Fukasawa, K., Paull, K.D., and van de Woude, G.F. (1998) Proteolytic inactivation of MAP-kinase-kinase by anthrax lethal factor. *Science.* 280, 734-737.
- Erwin, 2001. Erwin, J.L., DaSilva, L.M., Bavari, S., Little, S.F., Friedlander, A.M., and Chanh, T.C. (2001) Macrophage-derived cell lines do not express proinflammatory cytokines after exposure to *Bacillus anthracis* lethal toxin. *Infect Immun.* 69, 1175-1177.
- Fleming, 2009. Fleming, E.J., Hack, C.E., Robinson, P.J., and Gearhart, J.M. (2009) A physiologically based biokinetic (PBBK) model of systemic *Bacillus anthracis* toxins. International *Bacillus anthracis*, *B. cereus* and *B. thuringiensis* Conference, Santa Fe, NM, August 30 - Sept 3, 2009.
- Guidi-Rontani, 1999. Guidi-Rontani, C., Weber-Levy, M., Labruyere, E., and Mock, M. (1999) Germination of *Bacillus anthracis* spores within alveolar macrophages. *Mol Microbiol.* 31, 9-17.
- Gutting, 2005. Gutting, B.W., Gaske, K.S., Schilling, A.S., Slaterbeck, A.F., Sobota, L., Mackie, R.S., and Buhr, T.L. (2005) Differential susceptibility of macrophage cell lines to *Bacillus anthracis*-Vollum 1B. *Toxicol In Vitro.* 19, 221-229.
- Hack, 2009. Hack, C.E., Fleming, E.J., and Gearhart, J.M. (2009) A mathematical model of region-specific deposition of inhaled microorganisms in the rabbit lung.

International *Bacillus anthracis*, *B. cereus* and *B. thuringiensis* Conference, Santa Fe, NM, August 30 - Sept 3, 2009.

Huang, 1996. Huang, C.Y. and Ferrell, J.E. (1996) Ultrasensitivity in the mitogen-activated protein kinase cascade. Proc Natl Acad Sci USA. 93, 10078-10083.

Kholodenko, 2000. Kholodenko, B.N. (2000) Negative feedback and ultrasensitivity can bring about oscillations in the mitogen-activated protein kinase cascades. Eur. J. Biochem. 267, 1583-1588.

Leppla, 1995. Leppla, S.H. (1995) Anthrax toxins. In: Bacterial Toxins and Virulence Factors in Disease. Handbook of Natural Toxins, Vol. 8. (Eds. J. Moss, B. Iglewski, M. Vaughan and A. Tu) pp. 543–572. New York: Marcel Dekker.

Levchenko, 2000. Levchenko, A., Bruck, J., and Sternberg, P.W. (2000) Scaffold proteins may biphasically affect the levels of mitogen-activated protein kinase signaling and reduce its threshold properties. Proc Natl Acad Sci USA. 97, 5818–5823.

Moayeri, 2009. Moayeri, M. and Leppla, S.H. (2009) Cellular and systemic effects of anthrax lethal toxin and edema toxin. Mol Aspects Med. 30, 439-455.

Muehlbauer, 2007. Muehlbauer, S.M., Evering, T.H., Bonuccelli, G., Squires, R.C., Ashton, A.W., Porcelli, S.A., Lisanti, M.P., and Brojatsch, J. (2007) Anthrax lethal toxin kills macrophages in a strain-specific manner by apoptosis or caspase-1-mediated necrosis. Cell Cycle. 6,758-766.

Ono, 2000. Ono, K. and Han, J. (2000) The p38 signal transduction pathway; Activation and function. Cell Signal. 12, 1-13.

Park, 2002. Park, J.M., Greten, F.R., Li, Z.-W., and Karin, M. (2002) Macrophage apoptosis by anthrax lethal factor through p38 MAP kinase inhibition. Science. 297, 2048-2051.

Pellizzari, 1999. Pellizzari, R., Guidi-Rontani, C., Vitale, G., Mock, M., and Montecucco, C. (1999) Anthrax lethal factor cleaves MKK3 in macrophages and inhibits the LPS/IFN $\gamma$ -induced release of NO and TNF $\alpha$ . FEBS Lett. 462, 199-204.

Ribot, 2006. Ribot, W.J., Panchal, R.G., Brittingham, K.C., Ruthel, G., Kenny, T.A., Lane, D., Curry, B., Hoover, T.A., Friedlander, A.M., and Bavari, S. (2006) Anthrax lethal toxin impairs innate immune functions of alveolar macrophages and facilitates *Bacillus anthracis* survival. Infect Immun. 74, 5029-5034.

Robinson, 2009. Robinson, P.J., Fleming, E.J., Hack, C.E., and Gearhart, J.M. (2009) Multi-scale mechanistically-based *in silico* simulation of anthrax-host interaction: Modulation of macrophage map kinase signaling pathway by lethal toxin. International

*Bacillus anthracis*, *B. cereus* and *B. thuringiensis* Conference, Santa Fe, NM, August 30 - Sept 3, 2009.

Ross, 1957. Ross, J.M. (1957) The pathogenesis of anthrax following the administration of spores by the respiratory route. J. Pathol. Bacteriol. 73, 485-494.

Schneider 2008. Schneider, D.J. (2008) Three models of anthrax toxin effects on the map-kinase pathway and macrophage survival. Thesis, Air Force Institute of Technology, Wright-Patterson AFB, OH.

Vitale 1998. Vitale, G., Pellizzari, R., Recchi, C., Napolitani, G., Mock, M., and Montecucco, C. (1998) Anthrax lethal factor cleaves the N-terminus of MAPKKs and induces tyrosine/threonine phosphorylation of MAPKs in cultured macrophages. Biochem Biophys Res Commun. 248, 706-711.

## APPENDIX: MODEL SIMULATION (BERKELEY MADONNA™)

; (Comments are preceded by semi-colons)

MAPKK is represented by MKK

MAPKKK is represented by MKKK

; Reaction Rates J (units nM/s):

$$J1 = V1 * MKKK / ((1 + ((MAPK\_PP / Ki)^n)) * (K1 + MKKK))$$

$$J2 = V2 * MKKK\_P / (KK2 + MKKK\_P)$$

$$J3 = k3 * MKKK\_P * MKK / (KK3 + MKK)$$

$$J4 = k4 * MKKK\_P * MKK\_P / (KK4 + MKK\_P)$$

$$J5 = V5 * MKK\_PP / (KK5 + MKK\_PP)$$

$$J6 = V6 * MKK\_P / (KK6 + MKK\_P)$$

$$J7 = k7 * MKK\_PP * MAPK / (KK7 + MAPK)$$

$$J8 = k8 * MKK\_PP * MAPK\_P / (KK8 + MAPK\_P)$$

$$J9 = V9 * MAPK\_PP / (KK9 + MAPK\_PP)$$

$$J10 = V10 * MAPK\_P / (KK10 + MAPK\_P)$$

KX=0; This parameter (units  $s^{-1}$ ) is fitted to data (by eye, via slider)

JX = KX \* MKK; This represents cleavage of MKK by LF

JXP = KX \* MKK\\_P; This represents cleavage of MKK\\_P by LF

JXPP = KX \* MKK\\_PP; This represents cleavage of MKK\\_PP by LF

; Differential Equations:

$$MKKK' = - J1 + J2$$

$$MKK' = - J3 + J6 - JX; \text{ Where JX represents cleavage by LF}$$

$$MKK\_P' = + J3 - J4 + J5 - J6 - JXP; \text{ JXP is cleavage of MKK\_P by LF}$$

$$MAPK' = - J7 + J10$$

$$MAPK\_P' = + J7 - J8 + J9 - J10$$

$$MKKK\_P' = + J1 - J2$$

$$MKK\_PP' = + J4 - J5 - JXPP; \text{ JXPP is cleavage of MKK\_PP by LF}$$

$$MAPK\_PP' = + J8 - J9$$

; Initial Values (concentrations in nM)

$$\text{init MKKK} = 90; \text{ Total MKKK (MKKK + MKKK\_P)} = 100 \text{ nM}$$

$$\text{init MKKK\_P} = 10$$

$$\text{init MKK} = 280; \text{ Total MKK (MKK + MKK\_P + MKK\_PP)} = 300 \text{ nM}$$

$$\text{init MKK\_P} = 10$$

$$\text{init MKK\_PP} = 10$$

$$\text{init MAPK} = 280; \text{ Total MAPK (MAPK + MAPK\_P + MAPK\_PP)} = 300 \text{ nM}$$

$$\text{init MAPK\_P} = 10$$

$$\text{init MAPK\_PP} = 10$$

; Parameter Values

V1 = 2.5; maximum phosphorylation rate for MAPKKK (nM/s)

Ki = 9; (nM)

n = 1; Feedback sensitivity parameter (unitless)

K1 = 10; (nM)

V2 = 0.25; (nM/s)

KK2 = 8; (nM)

k3 = 0.025; (s<sup>-1</sup>)

KK3 = 15; (nM)

k4 = 0.025; (s<sup>-1</sup>)

KK4 = 15; (nM)

V5 = 0.75; (nM/s)

KK5 = 15; (nM)

V6 = 0.75; (nM/s)

KK6 = 15; (nM)

k7 = 0.025; (s<sup>-1</sup>)

KK7 = 15; (nM)

k8 = 0.025; (s<sup>-1</sup>)

KK8 = 15; (nM)

V9 = 0.5; (nM/s)

KK9 = 15; (nM)

V10 = 0.5; (nM/s)

KK10 = 15; (nM)

starttime = 0

stoptime = 90000

dtmin = 0.0001; minimum (and initial) step size

dtmax=10; maximum step size